

# One-week glucose control via zero-order release kinetics from an injectable depot of glucagon-like peptide-1 fused to a thermosensitive biopolymer

Kelli M. Luginbuhl<sup>1</sup>, Jeffrey L. Schaal<sup>1</sup>, Bret Umstead<sup>2</sup>, Eric M. Mastria<sup>1</sup>, Xinghai Li<sup>1</sup>, Samagya Banskota<sup>1</sup>, Susan Arnold<sup>2</sup>, Mark Feinglos<sup>3</sup>, David D'Alessio<sup>3</sup>, Ashutosh Chilkoti<sup>1\*</sup>

## Author Affiliations

<sup>1</sup> Department of Biomedical Engineering, Duke University, Durham, North Carolina 27708, USA

<sup>2</sup> PhaseBio Pharmaceuticals, Inc., Malvern, Pennsylvania 19355, USA

<sup>3</sup> Division of Endocrinology, Metabolism, and Nutrition, Duke University Medical Center, Durham, North Carolina 27710, USA

\* Author to whom correspondence should be addressed (email: [chilkoti@duke.edu](mailto:chilkoti@duke.edu))

## Supporting Information

### Table of Contents

1. Methods.....	S2
1.1 Construct sequencing information .....	S2
1.2 Iodination of GLP1-ELP .....	S2
1.3 Calculation of minimum effective concentration.....	S2
1.4 Preparation and validation of GLP1-ELP <sub>opt</sub> for non-human primate study .....	S2
2. GLP1-ELP Fusion Characterization .....	S5
2.1 Assessing purity with SDS-PAGE .....	S5
2.2 Hydrodynamic radius comparisons.....	S5
3. Short-term <i>In Vivo</i> Studies in Mice.....	S5
3.1 Early time points and intravenous injections .....	S6
3.2 Dose response .....	S7
3.3 Biodistribution .....	S8
3.4 Blood glucose returning to untreated levels.....	S8
3.5 Images from $\mu$ SPECT-CT.....	S8
3.6 Injection site histology .....	S10
4. Long-term <i>In Vivo</i> Studies in mice .....	S11
4.1 Blood glucose and HbA1c correlation .....	S11
4.2 Blood glucose regulation after repeated injections .....	S11
5. <i>In Vivo</i> Studies in Monkeys .....	S11
5.1 Immunogenicity .....	S11
5.2 Pharmacokinetics .....	S12

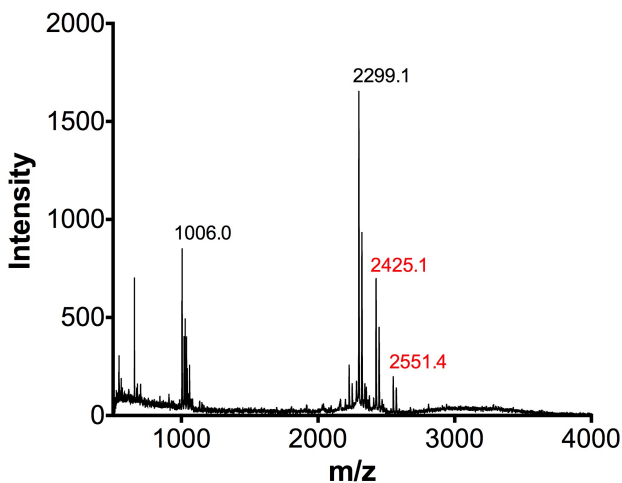
## 1. Methods

### 1.1 Construct sequencing information

The GLP1 used in all studies was a modified version, unless otherwise mentioned (as in the cAMP *in vitro* studies): AAHGEGTFTSDVSSYLEEQAAKEFIWLKVGAG. All ELPs were comprised of (VPGXG)<sub>n</sub> repeats where ‘X’ residue composition and ‘n’ number of repeats are listed in Table 1.

### 1.2 Iodination of GLP1-ELP

An identical procedure to that outlined in the Methods Section 2.6.4 was performed using non-radioactive NaI to iodinate the tyrosine residue of GLP1. After iodination and overnight dialysis in PBS, the concentrations were determined by measuring 280 nm absorbance on a NanoDrop 1000 and successful iodination was confirmed with matrix-assisted laser desorption and ionization mass spectrometry (MALDI-MS) on a trypsin digested sample (SI Figure 1). For the tryptic digest, samples were diluted to 25  $\mu$ M in 50 mM ammonium bicarbonate and incubated with 0.2  $\mu$ g MS grade trypsin (ThermoFisher Scientific) for 4 h at 37°C. Samples were diluted 1:10 in 10 mg/mL 4-hydroxycinnamic acid (HCCA) matrix prior to analysis with a DE-Pro MALDI-MS (Applied Biosystems). The two unmodified peaks, labeled in black, correspond to the expected peaks for digested, unmodified GLP1 (2299.4 and 1006.2 Da). The peaks labeled in red correspond to the 2299 Da peak modified with one and two iodines.



SI Figure 1. MALDI-MS of trypsinized GLP1 after labeling with iodine. Unmodified peaks for digested GLP1 are labeled in black and iodinated peaks are labeled in red.

### 1.3 Calculation of minimum effective concentration

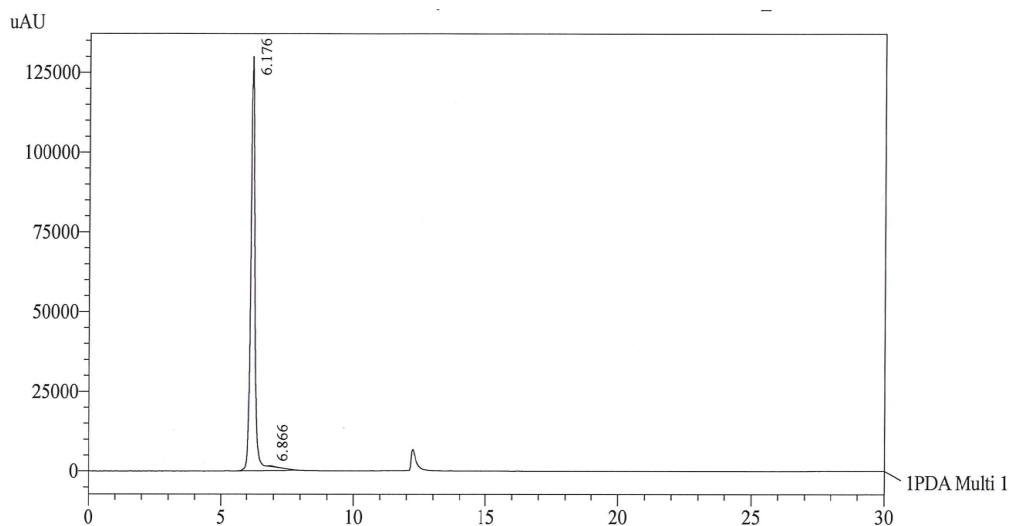
A minimum effective concentration for GLP1-ELPs was calculated using information published on how GLP1’s insulin-releasing effects are dependent on an intravenous dose in mice. A 0.3 nmol/kg dose leads to peak concentrations of approximately 100 pM<sup>70</sup>. In a separate study, a dose of between 3 and 10 nmol/kg GLP1 led to an abrupt increase in the second-phase of insulin release<sup>69</sup>. Using linear scaling, a 10 nmol/kg dose would reach peak concentrations in circulation of approximately 3.3 nM. By adjusting for the fusion’s 12-fold higher EC<sub>50</sub>, we calculated a minimal effective concentration to be roughly 40 nM.

### 1.4 Preparation and validation of GLP1-ELP<sub>opt</sub> for non-human primate study

#### 1.4.1 Assessment of purity with SEC-HPLC

Purified GLP1-ELP<sub>opt</sub> was analyzed with SEC-HPLC using 5% acetonitrile (ACN) in PBS isocratic flow as the mobile phase. The pump flow rate was set to 1 mL/m for a 30 m run time. The sample was diluted to 1 mg/mL in mobile phase and 50  $\mu$ L was injected. A total of three sample injections were performed. A 50  $\mu$ L mobile phase blank was also analyzed. The samples were detected with a photodiode array

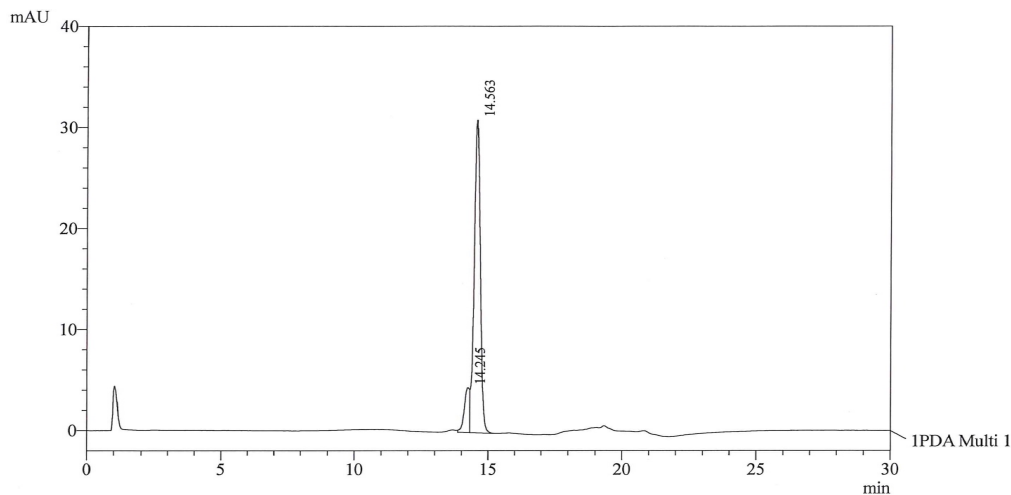
(PDA) at 280 nm (SI Figure 2). The average percent purity for GLP1-ELP<sub>opt</sub> was 99.67%. The chromatogram showed a small tailing peak of a smaller species off of the main peak for each of the three sample injections. There were no detected peaks in the blank.



SI Figure 2. SEC-HPLC of purified GLP1-ELP<sub>opt</sub> product.

#### 1.4.2 Assessment of purity with RP-HPLC

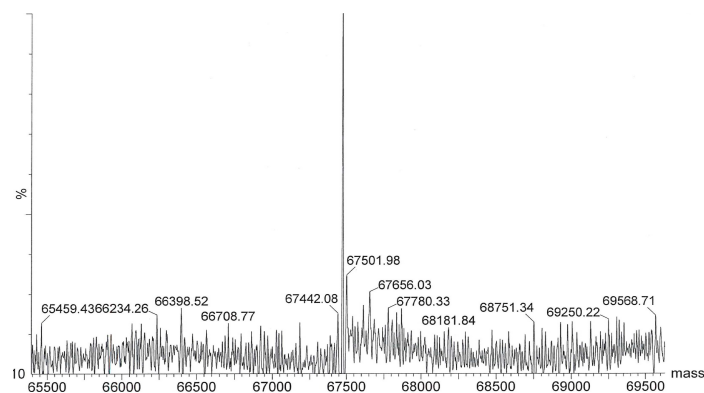
RP-HPLC was performed with a 1 mL/m flow rate using the following gradient: 20% ACN in water with 0.1% TFA increasing over a 30 m run time to 50% ACN in water with 0.1% TFA followed by a 100% ACN in 0.1% TFA wash to strip the column of all remaining molecules. Purified GLP1-ELP<sub>opt</sub> was diluted to 1 mg/mL in mobile phase and 50  $\mu$ L was injected. A total of three sample injections were performed in addition to a 50  $\mu$ L mobile phase blank. The samples were detected with a PDA at 280 nm (SI Figure 3). The average percent purity for GLP1-ELP<sub>opt</sub> was 89.02%. The chromatogram showed a front shoulder peak off of the main peak for each of the three sample injections. There were no detected peaks in the blank.



SI Figure 3. RP-HPLC of purified GLP1-ELP<sub>opt</sub> product.

### 1.4.3 Confirmation of the product's mass and sequence

Mass spectrometry was performed using a Micromass Q-ToF API US Quadrupole/Time-Of-Flight mass spectrometer. GLP1-ELP<sub>opt</sub> was desalted using a Waters MassPREP online desalting cartridge; the eluted sample was introduced into the instrument in 80% ACN in water with 0.1% formic acid. GLP1-ELP<sub>opt</sub> gave a positive ion electrospray-MS spectrum with a major series of possible multiply-charged ions. When deconvoluted, these data show a major component with a chemical average molecular mass of 67,474.7 Da (SI Figure 4), which corresponds to the theoretical MW within the range of the instrument's accuracy. The theoretical MW of GLP1-ELP<sub>opt</sub> is 67,607.6 Da with an N-terminal Met and 67,476.4 with the N-terminal Met cleaved post-translationally.



**SI Figure 4.** Mass spectrometry shows a major peak for the purified GLP1-ELP<sub>opt</sub> product at 67,474.7 Da.

Prior to sample analysis, GLP1-ELP<sub>opt</sub> was buffer exchanged into PBS using a Nanosep 10 k Spin Cartridge (Pall). Pulsed liquid-phase N-terminal sequencing was performed using an Applied Biosystems (ABI) 492 automatic protein sequencer. Seven cycles of Edman degradation were carried out with the ABI program; the major amino acids detected in each cycle are presented in SI Table 1. A major His peak was also seen in residue 1, however, this was attributed to the presence of histidine in the sample buffer.

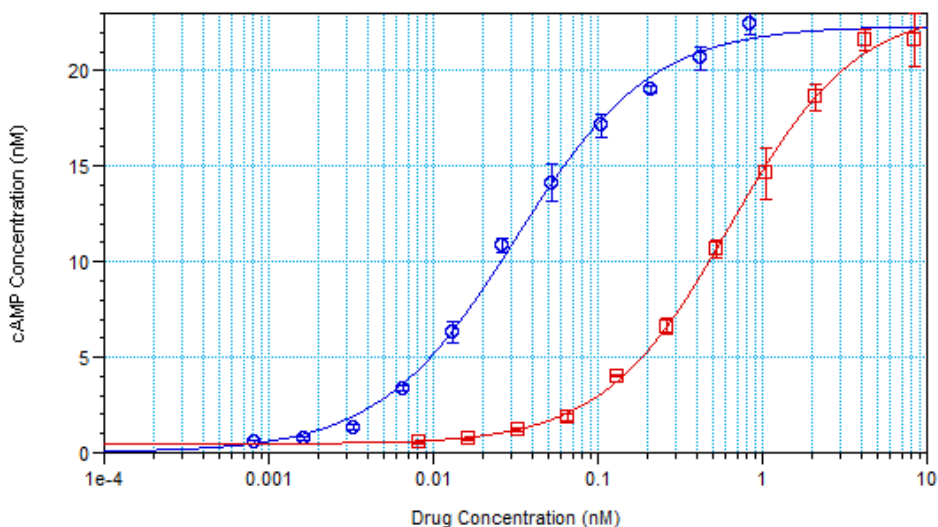
**SI Table 1.** N-terminal residues of GLP1-ELP<sub>opt</sub> detected by Edman Degradation.

Residue Cycle Number	Major Amino Acid Detected
1	Ala
2	Ala
3	His
4	Gly
5	Glu

### 1.4.4 Confirming purified product's activity

The day prior to the activity assay, GLP1R expressing Chinese hamster ovary (CHO) cells were plated on a 96-well tissue culture plate and incubated overnight at 37°C, 5% CO<sub>2</sub>. GLP1-ELP<sub>opt</sub> was incubated overnight with DPP-IV to cleave the Ala-Ala leader, yielding active peptide for receptor binding. Serial dilutions of native GLP1 control and GLP1-ELP<sub>opt</sub> were prepared in PBS. The cells were rinsed with Krebs-Ringer Bicarbonate Buffer (KRB) and then incubated at RT with 1 mM IBMX in KRB for 10 m to prevent cAMP degradation. The serial dilutions of samples were then added to the plate in duplicate and the plate was incubated at 37°C, 5% CO<sub>2</sub> for 20 m before lysing the cells to release cAMP. These samples and standards were added to the assay plate, followed by anti-cAMP antibody and competing HRP-cAMP; the plate was incubated at room temperature for 2 h. The plate was then washed and stoplight red substrate was added to each well and incubated 1 h at room temperature. The plate was read on a

fluorescence plate reader with 530 nm excitation, 590 nm emission, and a 570 nm cutoff. GLP1-ELP<sub>opt</sub> was determined to be 20.1 fold less active than GLP1 (SI Figure 5) based on the calculated EC<sub>50</sub> values.

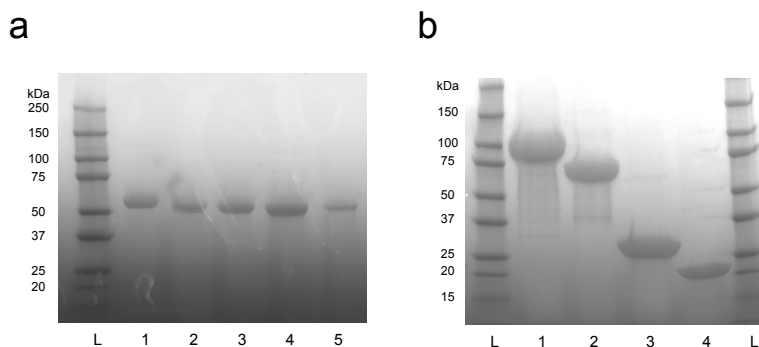


**SI Figure 5.** Assay measuring cAMP as an indicator of receptor activation for native GLP1 peptide (blue open circles) and GLP1-ELP<sub>opt</sub> (red open squares).

## 2. GLP1-ELP Fusion Characterization

### 2.1 Assessing purity with SDS-PAGE

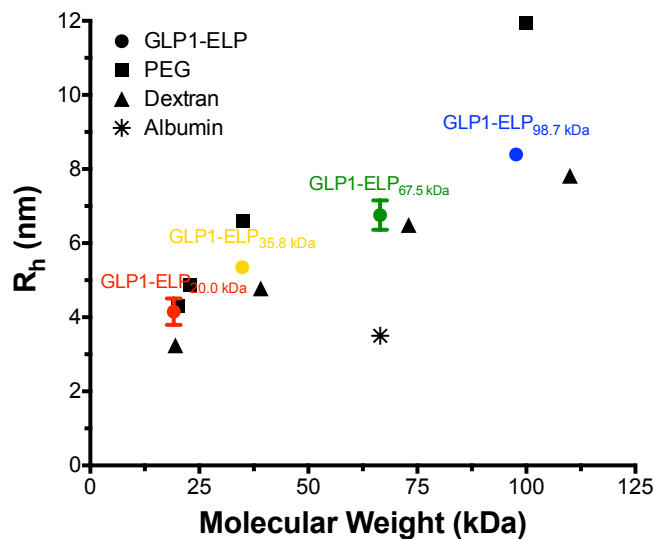
After purifying the GLP1-ELP fusions by ITC, we ran SDS-PAGE gel on 4-20% Tris gradient gels (Bio-Rad). To visually assess purity, these gels were negatively stained with 0.5 M CuCl<sub>2</sub> and the protein bands were compared to a standard ladder (Precision Plus Protein Kaleidoscope, Bio-Rad) to verify size.



**SI Figure 6.** SDS-PAGE gels of purified constructs with constant MW (a) or T<sub>i</sub> (b). Gels were run on 4-20% Tris-HCl at 180V for 48 min and stained with 0.5M CuCl<sub>2</sub>.

### 2.2 Hydrodynamic radius comparisons

The light scattering data for the GLP1-ELP series with varying MWs can be plotted alongside other hydrophilic, unstructured polymers, such as PEG and dextrans (SI Figure 7), which have similar hydrodynamic radii. The smallest fusion tested, GLP1-ELP<sub>20.0 kDa</sub> has an R<sub>h</sub> comparable to albumin. However, this construct had inferior pharmacokinetics. This could be explained by albumin's negative charge, which is believed to reduce its glomerular filtration in the kidneys, whose basement membrane is also negatively charged. In contrast, the ELP is comprised of uncharged residues.

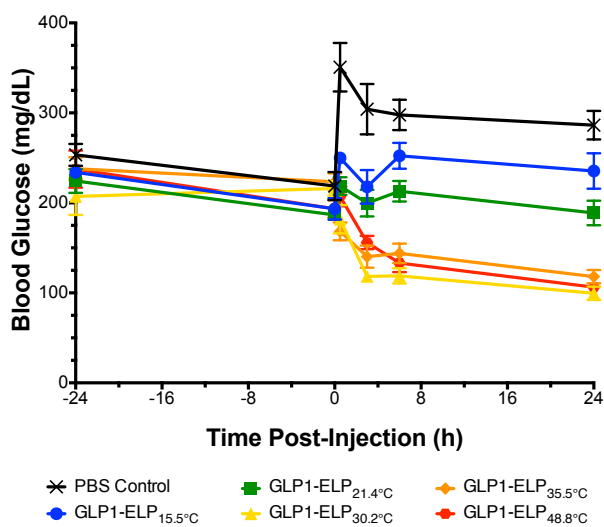


SI Figure 7.  $R_h$  values obtained by DLS plotted against MW for the set of GLP1-ELP fusions with variable MW in addition to values pulled from literature for linear PEG, dextran, and albumin.

### 3. Short-term *In Vivo* Studies in Mice

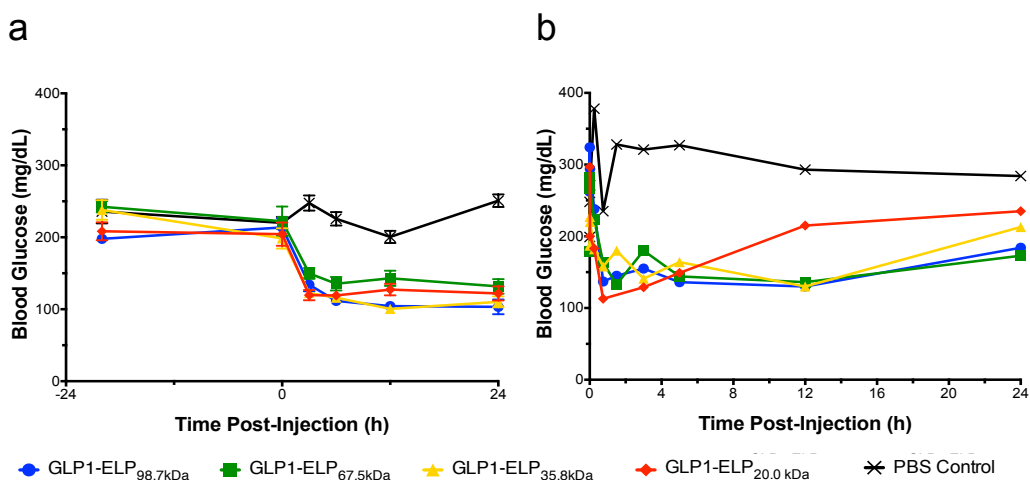
#### 3.1 Early time points and intravenous injections

DIO mice received a single, SC injection of either PBS or one of the GLP1-ELP fusions from the variable  $T_i$  series. Blood glucose was measured 24 h prior to injection and throughout the day after injection. SI Figure 8 serves as an inset to Figure 1d in the main body of the manuscript, making it easier to see the early time points.



SI Figure 8. Pre-treatment and day 1 blood glucose for GLP1-ELPs with variable  $T_i$ 's ( $n=5$ ).

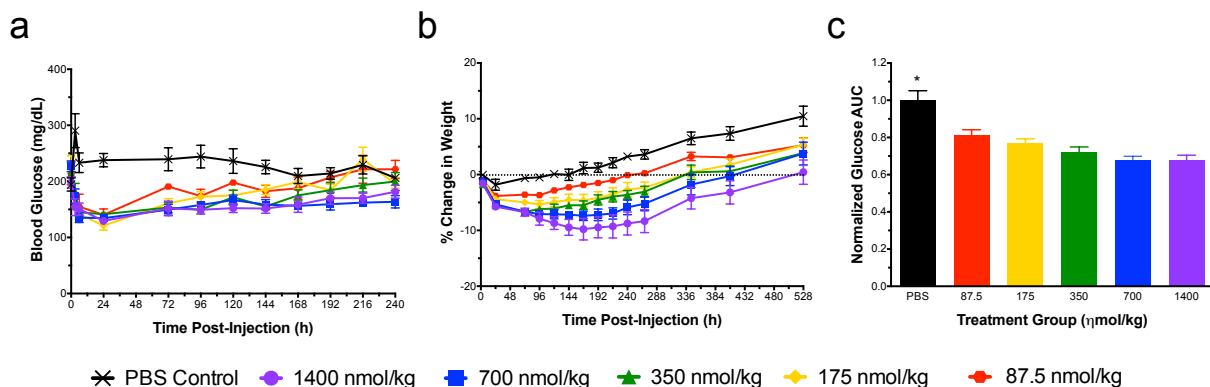
Similarly, SI Figure 9a, shows the same pre-treatment and day 1 blood glucose data for mice treated with either PBS or the series of GLP1-ELPs with variable MW. A small, pilot study was also conducted where mice were injected IV (10 nmol/kg at 1  $\mu$ M) with dilute GLP1-ELP fusions and blood glucose was subsequently monitored. The samples were diluted to a concentration at which the most hydrophobic fusion in the series did not transition at body temperature. IV injection removed the variable of depot-controlled release and isolated renal filtration. Even in this pilot study (n=1), it is apparent that GLP1-ELP<sub>20.0kDa</sub>, which had the worst performance after SC administration, is also cleared from the body the fastest (SI Figure 9b), likely owing to its free filtration due to its small size.



**SI Figure 9.** Pre-treatment and day 1 glucose data for the set of GLP1-ELPs with variable MW (n=6) (a) as well blood glucose levels in mice (n=1) receiving an intravenous (IV) injection of dilute GLP1-ELP bolus (b).

### 3.2 Dose response

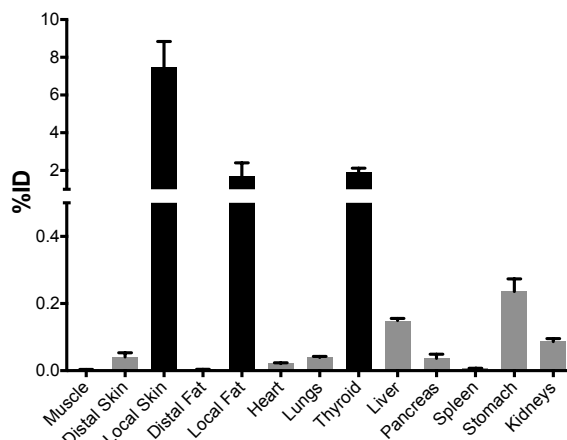
A dose response study using GLP1-ELP<sub>opt</sub> was conducted to determine the optimal once-weekly dose (SI Figure 10). Because the fusion's  $T_t$ , which has been optimized, is dependent on concentration, we kept concentration constant and instead varied injection volume. In our experience, injection volume has a much less significant impact on depot performance than  $T_t$ . Mice were injected with 87.5-1400 nmol/kg at 200  $\mu$ M with injection volumes ranging from about 20 to 270  $\mu$ L. Negative control mice were injected with PBS at volumes equivalent to the 1400 nmol/kg group. Because no further improvement in blood glucose was achieved with the 1400 nmol/kg dose (SI Figure 10a,c) and there was no statistically significant difference in weight change (SI Figure 10b), we selected 700 nmol/kg as the optimal dose.



**SI Figure 10.** Dose response study of GLP1-ELP<sub>opt</sub> in DIO mice (n=5) shows dose-dependence of blood glucose (a) and weight loss (b) effects with an optimal dose of 700 nmol/kg. There is a trend towards decreased glucose AUC with dose (c), but no difference between 700 and 1400 nmol/kg doses.

### 3.3 Biodistribution

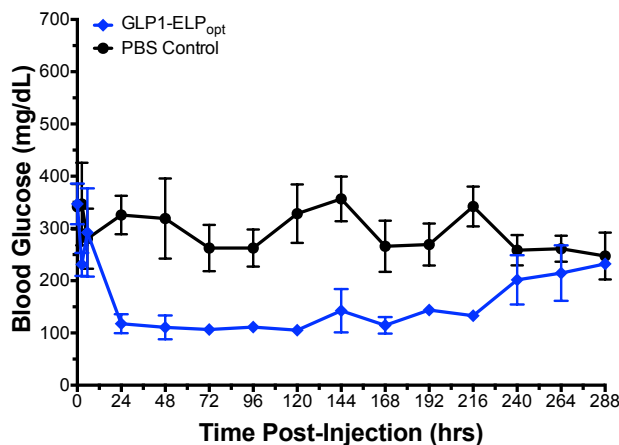
The ob/ob mice receiving treatment with radiolabeled GLP1-ELP<sub>opt</sub> were sacrificed on day 10 post-injection. At this time, relevant organs were excised and subjected to gamma counting to look at the fusion's biodistribution after 10 days of controlled release. The highest gamma counts, normalized to the injected dose, were found at the injection site and in the thyroid (SI Figure 11), which is unsurprising given its role in taking up iodine for hormone production. There was no significant accumulation in other vital organs, including those responsible for drug disposal – the kidneys and liver.



**SI Figure 11.** Day 10 biodistribution data for mice (n=4). Data is represented as mean percent injected dose (%ID) for each organ and SEM.

### 3.4 Blood glucose returning to untreated levels

For ob/ob mice treated with a single SC depot injection, blood glucose lowering effects are observed out to 10 d. Beyond 10 d, the mean blood glucose levels rises and is no longer statistically significantly different from the PBS treated control group (SI Figure 12).

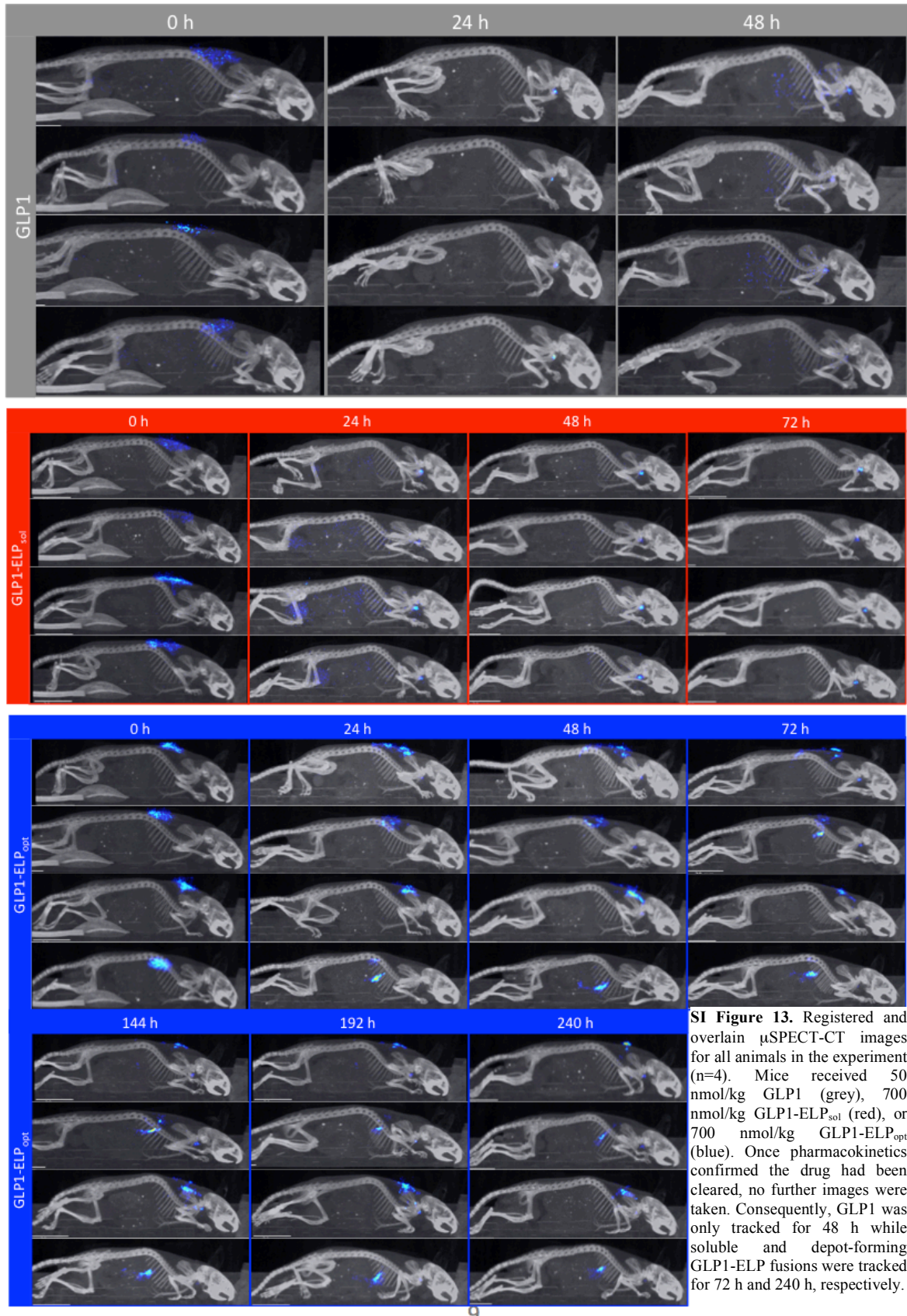


**SI Figure 12.** Extending the blood glucose versus time plot for ob/ob mice treated with either GLP1-ELP<sub>opt</sub> or saline shows that effects are no longer observed after 10 d post-injection.

### 3.5 Images from $\mu$ SPECT-CT

The main body of the manuscript presents registered  $\mu$ SPECT-CT images for a representative animal from each treatment group at time points relevant to the discussion. Below (SI Figure 13), we present images from all other mice across all time points at which images were collected.

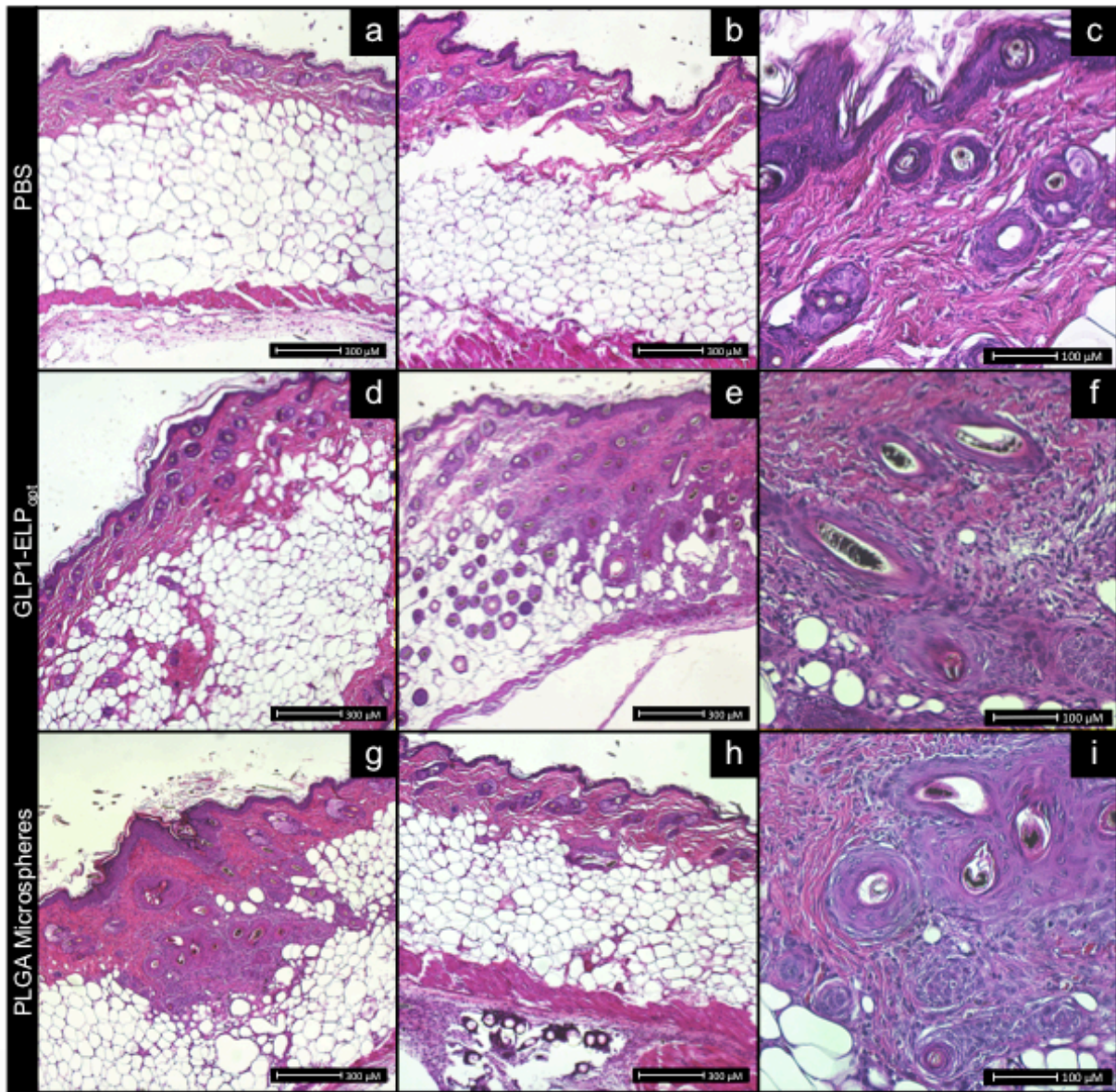






### 3.6 Injection site histology

Histology slides for skin from each mouse (SI Figure 14), injected with PBS, GLP1-ELP<sub>opt</sub>, or PLGA microspheres (n=3), were analyzed by a certified pathologist who was blinded to the group assignments. Nothing of interest was found in the PBS treated controls. In one GLP1-ELP sample, the pathologist found a focal apparent perifollicular fibrosis, which may have been due to the shaving methods, as well as mild histiocytic infiltrate. In all PLGA microsphere samples, there was evidence of mild to moderate histiocytic infiltrate. In one sample, there was also a spot of follicular fibrosis and a deep dermal/subcutaneous focus of fat necrosis. These histologic changes are consistent with the time frame of 5 days post-injection of foreign material. Because the GLP1-ELP<sub>opt</sub> samples looked no worse, if not better than PLGA microspheres (which are FDA approved for the delivery of a GLP1R agonist, exenatide), we are not concerned by any histologic findings.

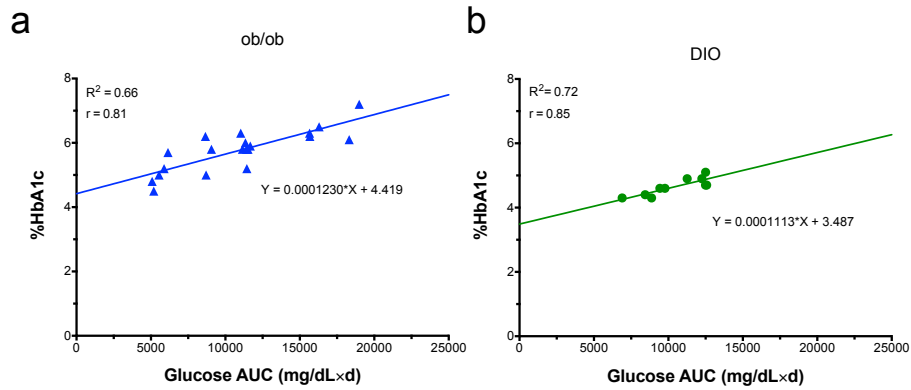


**SI Figure 14.** Representative histology of skin and subcutaneous tissue from the site of injection, stained with hematoxylin and eosin. Histological images are presented from mice injected with PBS (a-c), GLP1-ELP<sub>opt</sub> (d-f), and PLGA microspheres (g-i).

## 4. Long-term *In Vivo* Studies in Mice

### 4.1 Blood glucose and HbA1c correlation

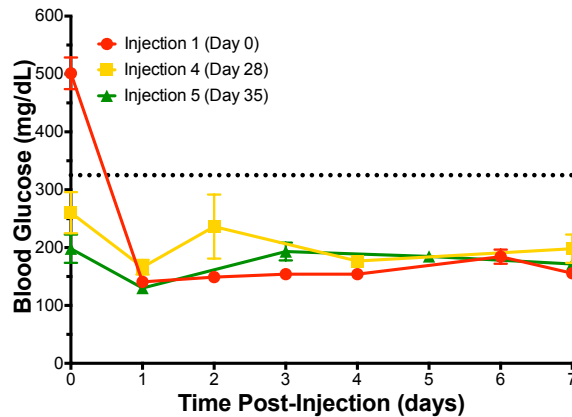
Over the course of an 8-week treatment regimen involving injections every 7 days in ob/ob mice and every 6 days in DIO mice, %HbA1c values are correlated to blood glucose exposure (AUC) (SI Figure 15).



**SI Figure 15.** %HbA1c is correlated with blood glucose AUC over the duration of long-term treatment. The correlation is present in both ob/ob (a) and DIO (b) mice.

### 4.2 Blood glucose regulation after repeated injections

We can overlay blood glucose data from different weeks through the course of the 8-week treatment. In DIO mice treated every 6 days with GLP1-ELP<sub>opt</sub>, there is no apparent reduction in efficacy at injections 4 and 5 compared to the first week of treatment (SI Figure 16). This provides indirect evidence against significant levels of circulating anti-drug antibodies, which would likely manifest as reduced efficacy with time.



**SI Figure 16.** Consistency of glycemic regulation with long-term treatment. Overlay of blood glucose profiles after injections 1, 4, and 5 in DIO mice receiving 700 nmol/kg GLP1-ELP<sub>opt</sub> every 6 days. Dotted line represents the PBS treated group's average blood glucose value.

## 5. *In Vivo* Studies in Monkeys

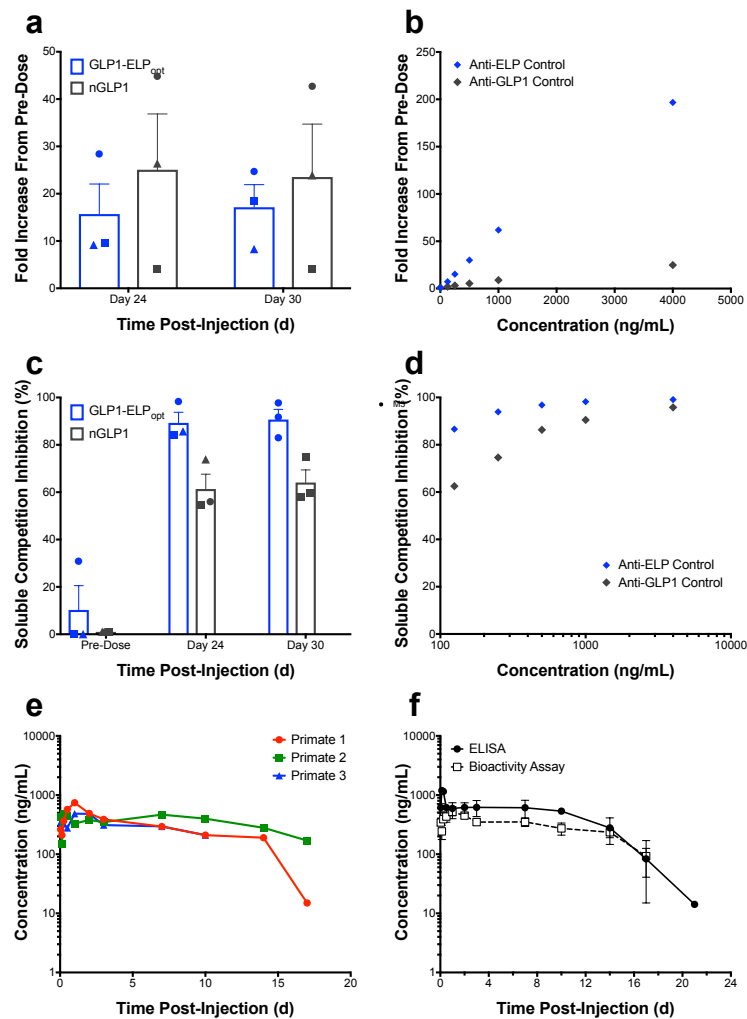
### 5.1 Immunogenicity

Cynomolgous macaques monkeys were injected with GLP1-ELP<sub>opt</sub> and blood was collected pre-injection as well as post-injection for 30 days. Anti-drug antibodies (ADAs) were measured by binding either GLP1-ELP<sub>opt</sub> or native GLP1 to a plate and quantifying the amount of bound mouse antibodies in the

serum at later time points (24 and 30 days) at which time, little to no drug remained in circulation. ADA measurement was done both with and without the addition of soluble, competitive drug or native GLP1 to determine specificity. Control measurements were made using dilutions of monoclonal mouse anti-GLP1 or polyclonal sheep anti-ELP. After measuring antibody binding as relative fluorescent units (RFUs), the data was presented as (1) fold-increase in RFU of day 24 and 30 serum over pre-dose samples (SI Figure 17 a-b) and (2) as % inhibition when assayed with soluble competition (SI Figure 17 c-d).

## 5.2 Pharmacokinetics

The serum samples were also used to assess pharmacokinetics by two methods: (1) a sandwich ELISA using anti-GLP1 and anti-ELP antibodies, and (2) a bioactivity assay by applying the serum to GLP1R expressing CHO cells and using cAMP production and a standard curve made by diluting drug in pre-dosing serum. Although ADAs were detected, the high correlation of the pharmacokinetics by bioactivity assay to the pharmacokinetics by ELISA (SI Figure 17e) suggests that these ADAs are not neutralizing.



**SI Figure 17.** Measuring anti-drug antibodies and bioactivity assay pharmacokinetics in non-human primates. Control antibodies and monkey serum samples at days 24 and 30 were compared to pre-dose samples for binding to drug (blue) and native GLP1 (black) both without (a-b) and with soluble competition by drug or native GLP1 (c-d). C Pharmacokinetics assessed by bioactivity assay (e) correlated well with pharmacokinetics as measured by ELISA (f). Circles, squares, and triangles represent primates 1, 2, and 3, respectively. Data represent mean and SEM.